

ORIGINAL RESEARCH PAPER

Evaluation of column studies using *Cynodon dactylon* plant-mediated amino-grouped silica-layered magnetic nanoadsorbent to remove noxious hexavalent chromium metal ions

Dhanya Vishnu  | Balaji Dhandapani 

Department of Chemical Engineering, Sri Sivasubramaniya Nadar College of Engineering, Chennai, India

Correspondence

Balaji Dhandapani, Department of Chemical Engineering, Sri Sivasubramaniya Nadar College of Engineering, Chennai, 603 110, India.
Email: balajid@ssn.edu.in

Funding information

SSN Trust, India

Abstract

Magnetic nanoparticles are desirable adsorbents because of their unique super-paramagnetic nature with the enhanced binding specificity and surface material interaction. The above unique features attract researchers to use it for wider applications. Herein, the study focuses on the amino-induced silica-layered magnetic nanoparticles amalgamated with plant-extracted products of *Cynodon dactylon* in order to turn them into a potent adsorbing material in a continuous column set up for the elimination of noxiously distributed Cr(VI) ions in the effluents. The selected plant-mediated magnetite nanoadsorbent, which was used in the fixed column studies, is optimised with the attributes of inlet concentration, adsorbent bed depth, and flow rate. Thomas, Yoon-Nelson and bed depth model showed the best experimental fit. Breakthrough adsorption time was reported for the various inlet concentrations of 100, 200 and 300 mg/L, adsorbent bed depths 2, 3 and 4 cm and volumetric flow rates of 4, 5 and 6 mL/min. The breakthrough point evaluated for the optimised attribute of inlet concentration of 100 mg/L, packed adsorbent depth 4 cm and flow rate 4 mL/min was 1400 min and the maximum removal efficiency was 60.6%. A better insight of the adsorption of metal ions for large-scale industrial effluents is provided.

1 | INTRODUCTION

Heavy metals account as the major pollutant and cause an imminent threat to the ecological communities in the ecosystem [1]. Their persistent and long-prevailing nature pollutes the atmosphere and poses an adverse health issue to the flora and fauna of the ecosystem [2]. Numerous health issues were addressed owing to the stack of heavy metal and intensification in the system [3]. Chromium is abundant in the environment as trivalent and hexavalent ions [4]. Trivalent chromium ions play a substantial role in balancing the insulin level and regulate the blood glucose content in the blood preventing diabetes [5, 6]. Hexavalent chromium considered as the noxious content tends to produce adverse health concerns on human consumption. International cancer research institutions have listed the severe effects of hexavalent chromium metal ions upon their

consumption [7]. Also, based on the human impact, the metal ion has been accounted as the group 1 category of human carcinogen. To prevent the impacts, the world health organisation has assigned the standard limit of chromium metal ions not to exceed beyond 0.05 mg/L [8].

The ample of conventional treatment methodologies such as membrane technologies, solvent extraction, oxidation/reduction, electrolysis treatment, adsorption, evaporative recovery, electro dialysis, by adding chemical precipitating agents, filtration, ion-exchangers and ultra-filtration, has been evaluated by many researchers to remove the heavy metal carcinogen from the ecosystem [9]. Adsorption was concentrated by many researchers around the world especially in the removal of the noxious heavy metallic constituents. The major advantage of this method was being competitive, simple and effective with low-cost strategy [10].

This is an open access article under the terms of the Creative Commons Attribution-NonCommercial-NoDerivs License, which permits use and distribution in any medium, provided the original work is properly cited, the use is non-commercial and no modifications or adaptations are made.

© 2021 The Authors. *IET Nanobiotechnology* published by John Wiley & Sons Ltd on behalf of The Institution of Engineering and Technology.

Nanotechnology is the promising discipline, and is quite used in the diversified applications owing to the unique characteristics feature of catalytic activity with the appropriate binding sites [8, 9]. Silver nanoparticles are blossomed in the market, owing to their excellent antimicrobial characteristics against several pathogens. The major disadvantage of regenerating capability prone the researchers to develop and reuse the magnetic particles [11]. Magnetic particles are reduced to nanosize particles and are incorporated with numerous polymeric substances and by-products of the microbial sources. These materials act as the multifaceted adsorbents and are used to remove the toxic metal constituents from the ecosystem [12, 13]. The preparation method for the metallic nanoparticle constitutes the usage of allergic chemical substances that elute the noxious secondary by-products to the environment [14].

The alternative approach developed by the researchers is to develop the metallic nanoparticles and to amalgamate them with numerous components of the plant system. This approach reduces the overall production cost and controls the elution of toxic secondary by-products in the ecosystem. The advantageous properties of superparamagnetic nature enhanced catalytic and stability features made to choose iron nanoparticle as the support [15]. Stability of the particle was further enhanced by coating silica substances to the exterior layer of the iron nanoparticles [16]. The polyphenolic components act as the prominent stabilizers and reduce the reacting molecules upon development of silver nanoparticle [17]. Most common usage of *Muraya koenigii* leaves in cooking is to increase the aroma of the food and thus acts as a popular flavouring material among the Indian people [18]. *Cynodon dactylon* plants are extensively found as weeds and are most commonly used to treat diabetes, asthma and inflammation owing to their enhanced antimicrobial feature of fighting against several pathogens.

The specific amino group was added to the surface of the silica-coated magnetic nanoparticle and plant-extracted products of *Cynodon dactylon* and *Muraya koenigii* were incorporated. Both the integrated biosorbent are utilised in the elimination of hexavalent chromium ions. The batch study was performed and it has been evaluated that the performance removal efficiency was more with nano-adsorbents prepared from *Cynodon dactylon* extracts and is explained in detail in our recent study [19]. In this study, column studies were evaluated, that propagates the scale-up of the system. The batch studies from the previous results are not sufficient for industrial application. The present study helps in the development of a fixed column using the above plant-integrated adsorbent to eliminate noxious hexavalent chromium metal ions. Few supportive literature in the column studies using plant-integrated nanoadsorbents are evaluated in the discharge of metal contaminants. The study emphasizes on achieving a reasonable high adsorption capacity in the presence of *Cynodon dactylon* integrated silica coated amino induced magnetic nanoadsorbents with an incomparable regenerating ability when compared with other studies.

2 | MATERIALS AND METHODS

Cynodon dactylon leaves, accumulated from Neyveli, India are immersed, dehydrated and sieved to get a desirable size of 150–1000 μm in the powdered form. The obtained powder was stored at 4°C for future use. About 1000 mg/L of the standard was prepared by dissolving potassium dichromate in the deionised water. Other chemicals used in this present study are listed as follows, ferrous sulphate ($\text{FeSO}_4 \cdot 7\text{H}_2\text{O}$), (3-amino-propyl) triethoxysilane (APTES), ferric chloride ($\text{FeCl}_3 \cdot 6\text{H}_2\text{O}$), tetraethyl orthosilicate (TEOS), ammonia and ethanol. All chemicals were obtained from SRL Chennai, India and were listed as analytical grade. pH adjustment was done with the aid of 0.1 M NaOH and 0.1 M HCl.

2.1 | Biosorbent preparation

Iron (III) chloride hexahydrate and ferrous sulphate heptahydrate were mixed in the ratio of 1:1 and dissolved in 100 mL of water. The mixture was processed with 20% ammonium hydroxide at a temperature of 60–65°C in the presence of nitrogen and thoroughly stirred for an hour. A black precipitate was obtained as the final product from the chemical reaction of the components that got settled at room temperature. The resultant black precipitate was cleaned with ethanol to eradicate other non-magnetic materials. The obtained magnetic product was dried at 90°C and mixed with 3 mL TEOS and 3 mL APTES. The mixed magnetic particles are allowed to react continuously for 8 h to coat themselves with silica during the silanisation process and to add the specific amino group [20]. The polyphenolic components extracted from the dried powder of *Cynodon dactylon* are added with the surface-modified amino induced silica-coated magnetic nanoparticles which are kept in the stirrer for 6 h at a temperature of 45–50°C [21]. The reacted mixture was allowed to settle for about 30 min. It is washed with ethanol to remove the non-magnetic material from the mixture. The above product was dried and separated under the aid of a strong magnetic power. The detailed characterisation studies were reported in our previous study [19]. The prepared nanoadsorbent was evaluated in the fixed column to eradicate noxious Cr (VI) metal ions. The metal ions were analysed with the aid of atomic absorption spectroscopy AAS (ELICO SL-176 Double beam AAS, India). All the analysis proceeded in triplets.

2.2 | Fixed bed column studies

The study was evaluated with the fixed column apparatus that has dimensions of 30 cm length and 2.56 cm internal diameter, respectively. The top and bottom of the column are filled with appropriate materials that act as a support for the adsorbent. The column was evaluated under different heights of the adsorbent (2, 3 and 4 cm) and the weight of the adsorbent differs based on the height of the adsorbing material packed in the column. Cr (VI) metal ion solutions corresponding to

concentrations of 100 mg/L, 200 mg/L and 300 mg/L are prepared and used in the column with varied flow rates of 4, 5 and 6 mL/min. The materials are prepared as stated above, and the simulated effluents are passed into the column and the effluents are collected at every 60 min to evaluate the noxious hexavalent chromium metal ions present in the solution using atomic absorption spectroscopy (AAS). The various parameters used in this study are given in Table 1, respectively. The desorption studies are also performed by introducing a regenerating agent into the exhausted adsorption bed. The treated noxious hexavalent chromium concentration was studied at several intervals using AAS. A 0.5-N NaOH solution was used as the regenerating agent in this study.

2.2.1 | Modelling of fixed bed adsorption in column studies

Breakthrough curve analysis

The performance study was evaluated for different feed flow of chromium concentrations (100, 200 and 300 mg/L) with varied heights (2, 3 and 4 cm) and flow rates (4, 5 and 6 mL/min). The breakthrough curve was analysed from the plot of $C_0/C_i V_s$ time. All the parameters obtained are from the below equation [22],

$$Q_{total} = \frac{Q}{1000} \int_{t=0}^{t=t_{total}} C dt \quad (1)$$

$$V_{total} = Q t_{total} \quad (2)$$

$$Q_{bed} = \frac{Q_{total}}{M} \quad (3)$$

$$M = (C_i * Q t_{total}) / 1000 \quad (4)$$

$$\% \text{Removal} = (Q_{total} / M) * 100 \quad (5)$$

where the above parameters are described and given below.

Q —Volumetric flow rate expressed in terms of (mL/min).

Q_{total} —Number of chromium ions adsorbed in the column and it was expressed in the terms of (mg).

C —Total chromium ions in the packed adsorbing material (mg/L).

V_{total} —Total effluent volume (mL).

Q_{bed} —nanoadsorbent capacity to adsorb Cr (VI) packed in the column and expressed in terms of (mg/g).

C_i —Concentration of the chromium metal ion passed through the inlet (mg/mL).

M —Total amount of chromium metal ions (mg).

2.2.2 | Thomas model

The Thomson model was used to determine the external and internal diffusion without any limitations during the adsorption process [23]. The equation was expressed in the linearised form as below [24],

$$\ln \left[\frac{C_i}{C_1} - 1 \right] = \frac{K_{th} Q_e M}{Q} - K_{th} C_i t \quad (6)$$

where the parameters are described as follows.

K_{th} determines the Thomas rate constant (mL/min.mg).

C_i —Concentration of the chromium metal ions passed through the inlet (mg/mL).

Q_e —adsorption capacity of chromium ions (mg/g)

M —Mass of the adsorbing material expressed in terms of (g).

Q —Volumetric flow rate (mL/min).

t —Total flow time (min).

C_1 —Effluent chromium ion concentration and is expressed in terms of (mg/mL). A graph was plotted for $\ln [(C_i/C_1)-1]$ and time (t), where Q_e and K_{th} represent the intercept and slope respectively.

2.2.3 | The Adams-Bhorat model

This model predicts the surface interaction that occurs between the surface of the adsorbent and the solute particles that bind to the adsorbent. The parameters K and N_0 were obtained from the graph plotted between bed height and the

TABLE 1 Influence on the process parameters used in the breakthrough curve analysis

	Parameters	t_b (min)	V_t (mL)	t_{total} (min)	m_{total} (g)	q_{total} (mg)	q_{bed} (mg/g)	%Removal
Inlet concentration of Cr (VI) ions (mg/L)	100	1400	17,250	3650	1725	1047.97	209.2	60.6
	200	800	12,500	2500	2500	1118.03	223.6	44.7
	300	500	10,500	2100	3150	1260	252	40
Bed depth (cm)	2	700	11,200	2240	1120	520	173.3	46.4
	3	800	14,200	2840	1420	800	200	56.3
	4	1400	17,250	3650	1725	1047.97	209.2	60.6
	4	1400	17,250	3650	1725	1047.97	209.2	60.6
Flow rate (mL/min)	4	1400	17,250	3650	1725	1047.97	209.2	60.6
	5	800	16,100	2683	1610	900	204	55.9
	6	600	15,200	2171	1520	770	168	50.6

total time. BDST was calculated from the below equation as follows [25],

$$t = \frac{N_0 Z}{C_i V} - \frac{1}{C_i K} \ln \left(\frac{C_i}{C_b} - 1 \right) \quad (7)$$

The simplified equation pioneered as,

$$t = aZ - b \quad (8)$$

'a' is defined as,

$$a = \frac{N_0}{C_i V} \quad (9)$$

$$b = \frac{1}{C_0 K} \ln \left(\frac{C_i}{C_b} - 1 \right)$$

where the parameters are ascribed as given below.

C_0 —inlet concentration of the chromium metal ions expressed in (mg/L).

V —flow velocity expressed in terms of (cm/min)

C_b —breakthrough concentration of the chromium metal ions expressed in terms of (mg/L).

N_0 —Bed adsorption capacity expressed in terms of (mg/L)

Z —Bed height (cm)

K —rate constant (L/mg min).

2.2.4 | Yoon–Nelson model

This model predicts the single component parameter without numerous operating parameters. The equation is given as follows [26],

$$\ln \left(\frac{C_1}{C_i - C_1} \right) = K_{yn} t - K_{yn} \tau \quad (10)$$

This method is to predict that the probability in the process rate declines concerning the breakthrough point of the chromium ions adsorbed on the adsorbent. The graph was plotted between $\ln(C_1/C_0 - C_1)$ and t . K_{yn} determined from the graph slope and the intercept gives $-\tau K_{yn}$.

3 | RESULTS AND DISCUSSION

3.1 | Parametric influence on column studies

Fixed-bed column studies calculated for various chromium concentrations of 100 mg/L, 200 mg/L and 300 mg/L with a bed height of 4 cm at a flow rate of 4 mL/min. From Fig (1), breakthrough and exhaustion time could be determined for the differed concentration range.

It was inferred that, at the lower chromium concentration, the breakthrough curve was attained at a longer period,

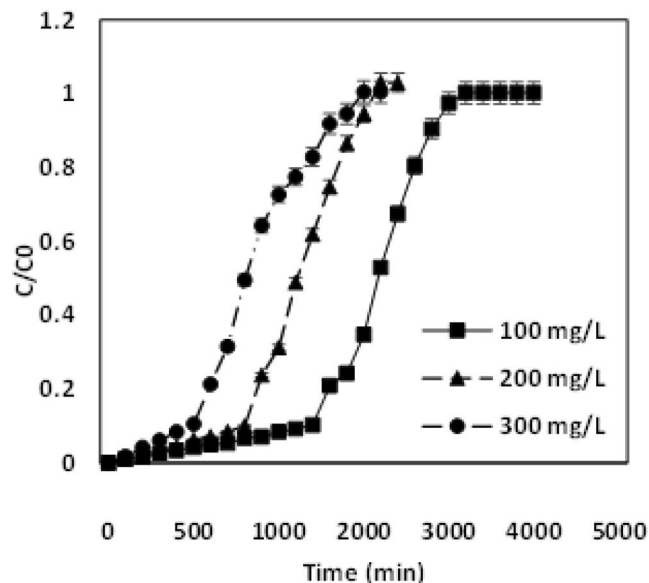


FIGURE 1 Breakthrough curve analysis for the adsorption of chromium at different concentration ranges of 100 mg/L, 200 mg/L and 300 mg/L

whereas the rise in concentration chromium ions reduced the breakthrough curve. The breakthrough curve for 100 mg/L was observed at 1400 min, whereas for the higher concentration gradients of 200 mg/L and 300 mg/L, breakthrough curve was observed at 800 and 500 min respectively. Due to the enhanced driving force at the enhanced concentration, the mass transfer resistance at the liquid phase was restricted. This leads to the fast binding of the metals to the adsorbent binding site within a short duration. A similar trend was compared and evaluated in other studies [27]. Thus, the breakthrough curve for the higher concentration gradient was attained in a shorter than the lower metal ion inlet concentration. From Fig (2), the breakthrough and exhaustion time could be determined for differed bed heights. Fig (2) depicts the effect of chromium ions into the adsorbent with the change in heights of 2, 3 and 4 cm for the inlet concentration of 100 mg/L and a volumetric flow rate 4 mL/min. Enhanced packed material height leads to a longer time duration to attain the breakthrough time [28].

The breakthrough time for 2 cm was attained at 700 min, whereas at varied heights of 3 and 4 cm the breakthrough time was determined at 800 and 1400 min. The increase in bed height causes increased saturation and exhaustion time. The availability of abundant binding capacity enhances chromium metal ion interaction with the adsorbent [22]. Fig (3) demonstrates the adsorption of chromium ions into the adsorbent with a change in the volumetric flow rate of 4, 5 and 6 mL/min for the inlet concentration of 100 mg/L and packed height of 4 cm. The breakthrough curve was attained in a short duration at a low flow rate, whereas the increase in flow rate decreases the breakthrough curve and exhaustion time [29]. The breakthrough curve was observed at 1400 min at a flow rate of 4 mL/min, whereas for 5 and 6 mL/min, the breakthrough time observed at 800 and 600 min, respectively. At a lower flow rate, the adsorption bed saturation takes more time,

since the gradient saturation sites are with less effective metal uptake [30]. The breakthrough curve prediction and their effect of various parameters are ascribed in Table 1. From the results of graph and table, the study evaluates higher efficiency removal of 60.6% with 209.2 mg/g of chromium that was adsorbed into the adsorbent. However, the removal efficiencies decreases to about 44.7% and 40% with the adsorption capacities of 223.6 mg/L and 252 mg/L for higher inlet concentrations of 200 mg/L and 300 mg/L chromium appropriately. Removal efficiencies for the lower depths of 2 and 3 cm were determined to be 46.4% and 56.3% and it was

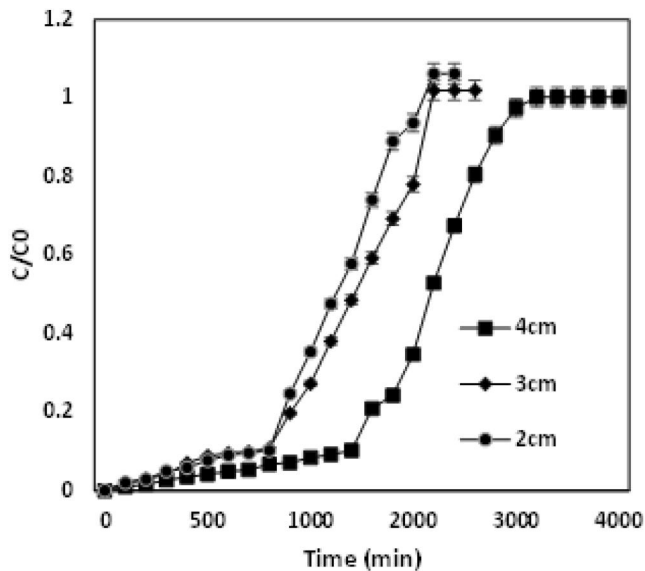


FIGURE 2 Breakthrough curve analysis for the adsorption of Cr (VI) metal ions with different heights of the bed—2, 3 and 4 cm for 100 mg/L

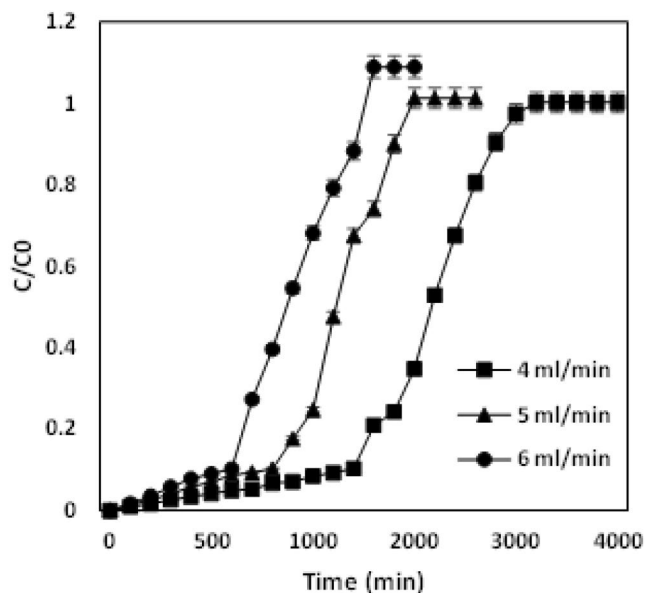


FIGURE 3 Breakthrough curve analysis for the adsorption of noxious chromium metal ions with different volumetric flow rates of 4, 5 and 6 mL/min for the inlet concentration range of 100 mg/L

comparatively lower than the removal efficiency of bed height 4 cm that was attributed to being 60.6 % respectively. The adsorption capacity was also higher for the enhanced bed height of 4 cm (209.2 mg/g) when related to the lower bed adsorbing material heights of 2 and 3 cm (173.3 mg/g, 200 mg/g). Subsequently, the removal efficiency evaluated at lower flow rate 4 mL/min was calculated as 60.6% with the adsorption capacity of 209.2 mg/g when compared with high flow rates of 5 and 6 mL/min which have removal efficiencies of about 55.9% and 50.6% with adsorption capacities of 204 and 168 mg/g respectively. The contact between an adsorbent and chromium ions are more at a reduced flow rate, enhanced bed adsorbing material height and at the reduced inlet concentration, which results in the numerous interaction between them. The diffusion phenomena enable more chromium adsorption in the surface of the adsorbent [22].

3.2 | Column data modelling

3.2.1 | Thomson model

Thomson model evaluates the adsorption capacity and the breakthrough curve based on the studies from the pseudo-second-order kinetics model and Langmuir isotherm. Subsequently, they follow the negligible resistances that occur throughout the system [22]. From the study, Q_0 adsorption capacity of the column and the Thomson constant K_{th} are calculated. The data modelling was predicted for the various metal-ion concentrations from 100 mg/L to 300 mg/L, bed depth heights 2, 3 and 4 cm and flow rate variations of 4, 5 and 6 mL/min. High R^2 value affirms the column model validity. Figure 4 describes the model data obtained for chromium

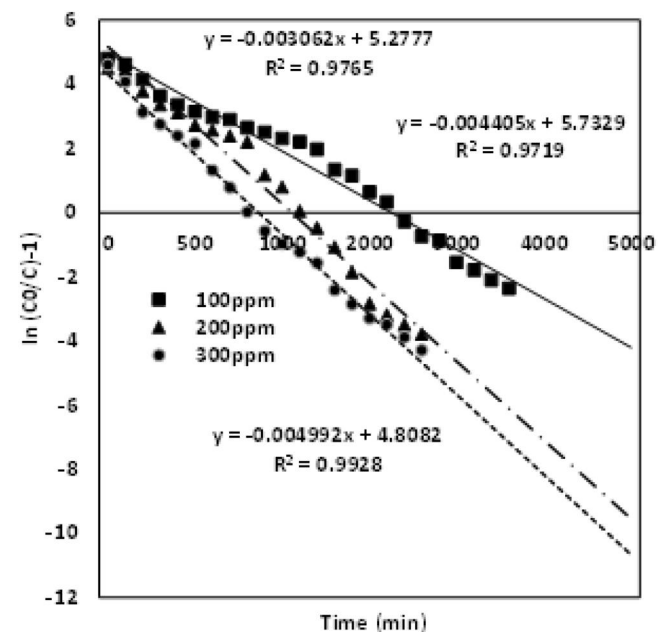


FIGURE 4 Thomson model validation for the various Cr (VI) concentrations of 100 mg/L, 200 mg/L and 300 mg/L

TABLE 2 Column modelling data for Thomson, Yoon-Nelson and bed depth service model

Model	Parameters	100 mg/L 4 cm 4 mL/min	200 mg/L 4 cm 4 mL/min	300 mg/L 4 cm 4 mL/min	100 mg/L 2 cm 4 mL/min	100 mg/L 3cm 4 mL/min	100 mg/L 4 cm 4 mL/min	100 mg/L 4 cm 4 mL/min	100 mg/L 4 cm 5 mL/min	100 mg/L 4 cm 6 mL/min
Thomson model	K_{th}	0.00003	0.00004	0.000045	0.00004	0.00003	0.00003	0.00003	0.000037	0.000048
	Q_0	172.10	143.25	120	119	134.85	172.10	172.10	127.02	92.5
	R^2	0.977	0.9719	0.9929	0.97	0.94	0.977	0.977	0.96	0.97
Yoon-Nelson model	K_{yn}	0.0033	0.004	0.005	0.0036	0.0043	0.0033	0.0033	0.0043	0.0052
	τ	1691.13	1180.7	943.25	1162.79	1333.33	1691.13	1691.13	1209	980.76
	R^2	0.95	0.96	0.99	0.97	0.95	0.95	0.95	0.94	0.98
Bed depth service model	K	0.0000372	0.0000446	0.000073	-	-	-	-	-	-
	N_0	3333.3	10,000.09	16,667.5	-	-	-	-	-	-
	R^2	0.99	0.99	0.99	-	-	-	-	-	-

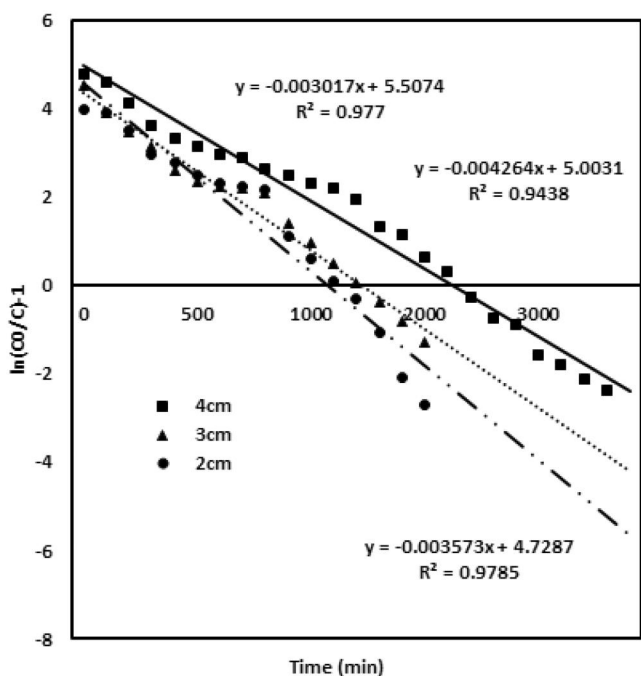


FIGURE 5 Thomson model validation for the different adsorbent bed heights of 2, 3 and 4 cm

concentrations of 100, 200 and 300 mg/L with a bed adsorbing material of height 4 cm and flow rate 4 mL/min.

The K_{th} value increases with enhanced concentration of noxious chromium metal ions, and the adsorption capacity Q_0 (172.1 mg/g) increases for the lower concentration of chromium ions (100 mg/L) when compared with higher concentrations of 200 mg/L (Q_0 —143.25 mg/g) and 300 mg/L (Q_0 —120 mg/g). The values are ascribed in Table 2. Figure 5 evaluates the model data obtained for different packed material heights of 2, 3 and 4 cm with chromium concentration of 100 mg/L and flow rate 4 mL/min. The K_{th} value for this model decreases for the

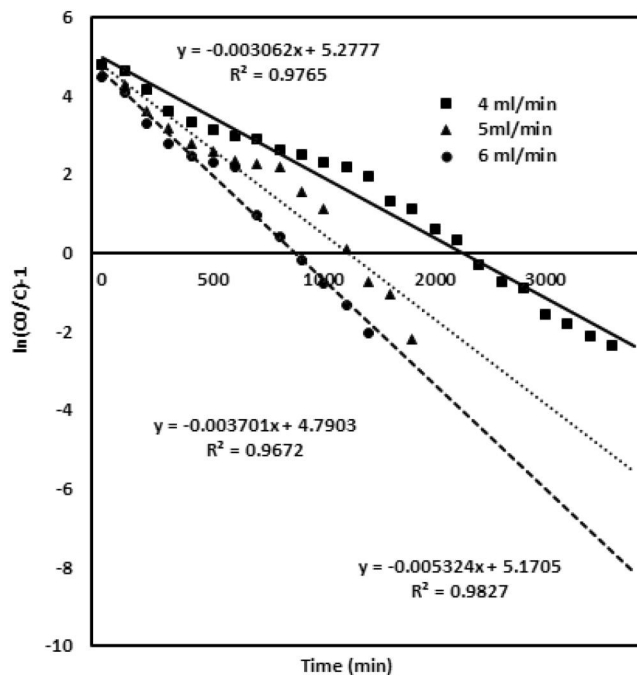


FIGURE 6 Thomson model validation for different flow rates of 4, 5 and 6 mL/min

enhanced bed height of the adsorbent, the adsorption capacity enhances with the upsurge in the bed height, while the values of K_{th} and Q_0 are given in Table 2. Figure 6 describes the model data examined for the various flow rates of 4, 5 and 6 mL/min with the chromium concentration of 100 mg/L and adsorbent packed material height of 4 cm. K_{th} and Q_0 observed for the flow rate follow an increasing trend for enhanced flow rate. The values are given in Table 2. The Thomas modelling trend demonstrates that the adsorption phenomena is not restricted by the chemical interaction, whereas it was governed by the surface interfacial mass transfer reaction [29]. More driving force was

required for the binding of adsorbent and the adsorbate at an enhanced chromium metal ion concentration [22]. This leads to an increased adsorption capacity at a lower concentration and flow rate. Subsequently, this model was validated due to high R^2 value and optimised column parameters of inlet concentration 100 mg/L, bed adsorbing material height 4 cm and flow rate of 4 mL/min which are preferred for maximised column performance.

3.2.2 | Yoon-Nelson model

The Yoon-Nelson model was evaluated for various parameters of chromium metal ion inlet concentration, packed height of the adsorbing material and the flow rates [27]. The results given in table (2) and the values of τ and K_{yn} are calculated from the graph. Figure 7 describes the model data obtained for the chromium concentration of 100, 200 and 300 mg/L with the bed adsorbing material height 4 cm and a flow rate of 4 mL/min. Figure 8 evaluates the model data obtained for the different bed heights of 2 cm, 3 and 4 cm with 100 mg/L chromium concentration and a flow rate of 4 mL/min. Figure 9 describes the model data examined for the various flow rates of 4, 5 and 6 mL/min with 100 mg/L chromium concentration and 4 cm adsorbent bed height. High correlation coefficient R^2 value predicts the satisfactory validation of this model. The values of both τ and K_{yn} from the table infer that both are inversely related to each other in the modelling equation. All the values are ascribed in the table. The rate constant increases and the τ value decreases upon enhanced inlet concentration and flow rates. At the enhanced inlet concentration, uptake of chromium metal ions by the

adsorbing material rapidly increases due to the availability of metal ions and binding sites [22].

This leads to rapid attainment of saturation point that declines the breakthrough curve of the adsorbate. However, on increase in bed height, τ value raises, since the establishment of more time between the adsorbent and the chromium metal ions occurs at the increased depth of the adsorbent.

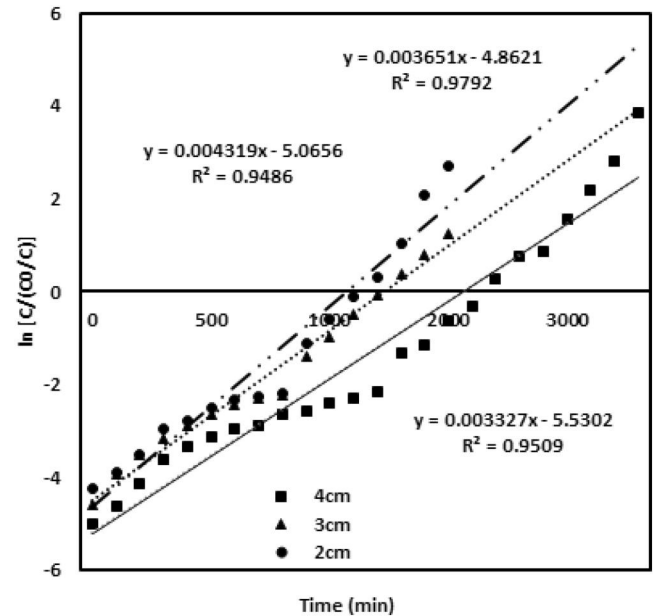


FIGURE 8 Yoon-Nelson model validation for different adsorbent bed heights of 2, 3 and 4 cm

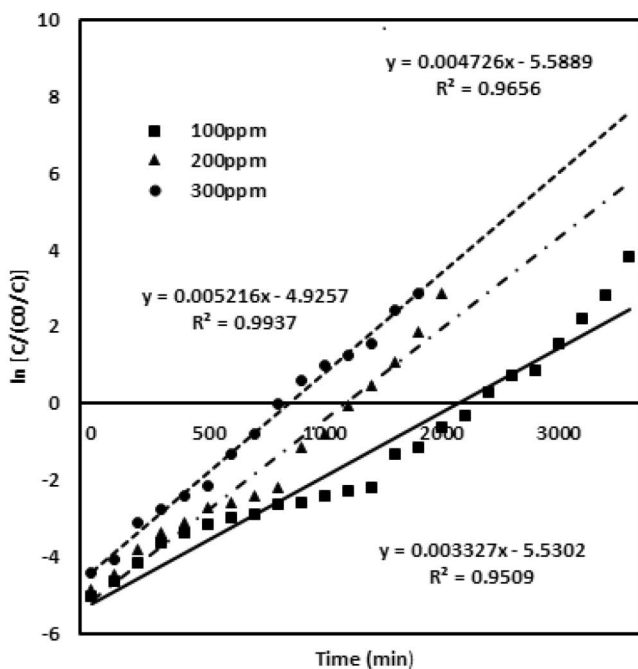


FIGURE 7 Yoon-Nelson model validation for various Cr (VI) concentrations of 100 mg/L, 200 mg/L and 300 mg/L

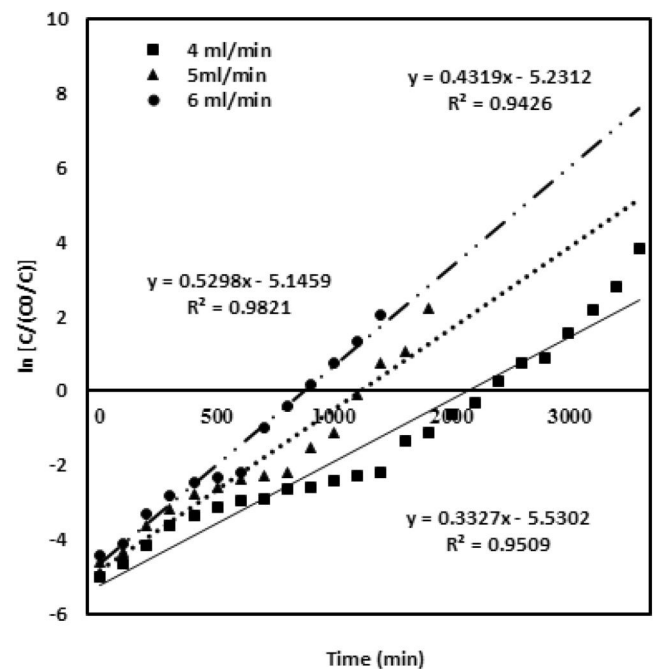


FIGURE 9 Yoon-Nelson model validation for different flow rates of 4, 5 and 6 mL/min

3.2.3 | The Bohart-Adams model

The Bohart-Adams model helps to determine the fundamental relationship between the C_0/C and t in a column study a phenomenal approach. This model evaluates the total service time for the adsorbent bed to be saturated and exhausted [31]. It is the most important pivotal parameter for scale-up studies. The model assumption follows surface reaction theory, where the reaction rate and the adsorption capacity of the chromium metal ions are directly related to each other. The study was carried out for the ratio of outlet to inlet concentration at a fixed flow rate. Figure 10 helps to determine the N_0 and K values and the values are ascribed in the table. It was inferred from the experimental data, that with the enhanced capacity of the adsorbent in the column, N_0 increases from 3333 to 16,667 mg/L. The more number of the adsorption binding sites results in the increased binding of chromium metal ions with the adsorbent. The correlation coefficient value R^2 is greater for this model and assumes a perfect approach to be carried on [32].

3.3 | Regenerative ability

The regenerative and reusing capability of the adsorbent is the main characteristic feature of the magnetic modified adsorbents [34, 38]. The reusable nature of the adsorbent was conducted with the experimental conditions of 100 mg/L chromium metal ion concentration, adsorbent bed depth of 4 cm and the flow rate of 4 mL/min. About 0.5 N NaOH was used as the regenerative agent after the completion of each cycle. Regeneration efficiency was calculated based on the ratio of the adsorption capacity after regeneration (Q_r) to the adsorption capacity at the original phase of the column (Q_0).

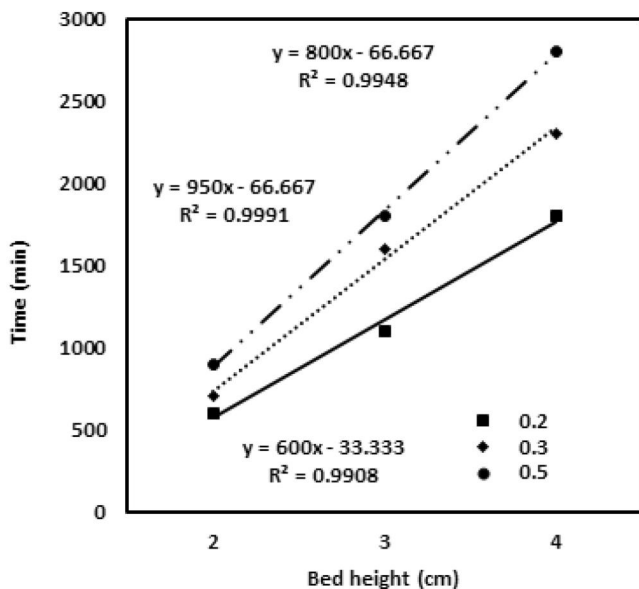


FIGURE 10 The Bohart-Adams model validation for the different inlet-outlet concentration

The adsorption and desorption studies are performed for the appropriate consequent four cycles. The breakthrough curve decreases after each consecutive cycle. The efficiency after each cycle was calculated as 69.06%, 51.51%, 43.5% and 28.97%. From the above results it is inferred that the prepared adsorbent was to discharge chromium ions from polluted effluents.

Comparative studies on the removal of chromium metal ions using various adsorbents [18] have been performed. From Table 3 results infer that prepared plant integrated nano-adsorbents possess enhanced adsorption capacity and are highly comparable with other adsorbents reported in studies. The study also reveals the regenerative ability of the adsorbent that helps with the scale-up process in the industries. The bed height used in the current study is highly remarkable when compared with other studies in the literature.

4 | CONCLUSION

The current study infers that the plant-mediated amino-functionalised silica-coated magnetic nanoadsorbent is a remarkable material to discharge noxious chromium metal ion content. Detailed evaluation was made in continuous fixed-bed column operations at various influenced parameters. The influential parameters were optimised under the inlet concentration of 100 mg/L with a sorbent packed height of 4 cm and the flow rate of 4 mL/min. Breakthrough curve analysis reveals that contact and saturation time were more for the initial concentration with minimal flow rate and the enhanced bed depth. Results of a batch study from our previous batch mode get correlated well with this column mode. The modelling data shows that both the Thomson model and Adams-Bohart model shows an excellent fit with experimental results. Thomson model affirms the process to

TABLE 3 Comparative study of the robust integrated biosorbent in the column studies to remove chromium ions

Adsorbing material	Adsorption capacity—chromium (mg/g)	Regenerative capacity	References
Modified Lagerstroemia bark	23.88	Five cycles	[33]
<i>Psidium guajava</i> leaves	8.72	-	[34]
Modified <i>Lantana camara</i>	362.8	Three cycles	[22]
Mango leaves	69.52	-	[35]
Chitosan nanofibre	360.1	Five cycles	[36]
Silica microspheres	57.78	-	[37]
<i>Cynodon dactylon</i> plant-mediated amino-functionalised silica-coated magnetic nanoadsorbent	209.02	Four cycles	Present study

follow monolayer adsorption that was correlated with the Langmuir model of the previous study batch.

ORCID

Dhanya Vishnu  <https://orcid.org/0000-0001-7607-2842>

Balaji Dhandapani  <https://orcid.org/0000-0002-4561-2022>

REFERENCES

1. Thekkudan, V.N., et al.: Review on nanoadsorbents: a solution for heavy metal removal from wastewater. *IET Nanobiotechnol.* 11(3), 213–224 (2017)
2. Sahraei, R., Ghaemy, M.: Synthesis of modified gum tragacanth/graphene oxide composite hydrogel for heavy metal ions removal and preparation of silver nanocomposite for antibacterial activity. *Carbohydr. Polym.* 157, 823–833 (2017)
3. Zhang, W., et al.: Synthesis of water-soluble magnetic graphene nanocomposites for recyclable removal of heavy metal ions. *J. Mater. Chem.* 1(5), 1745–1753 (2013)
4. Wang, Y.-T., Chirwa, E.M., Shen, H.: Cr(VI) reduction in continuous-flow coculture bioreactor. *J. Environ. Eng.* 126, 300–306 (2000)
5. Preuss, H.G., et al.: Comparing metabolic effects of six different commercial trivalent chromium compounds. *J. Inorg. Biochem.* 102(11), 1986–1990 (2008)
6. Baalamurugan, J., et al.: Slag-based nanomaterial in the removal of hexavalent chromium. *Int. J. Nanosci.* 17(1–2), 2–7 (2018)
7. Zou, Y., et al.: Environmental remediation and application of nanoscale zero-valent iron and its composites for the removal of heavy metal ions: a Review. *Environ. Sci. Technol.* 50(14), 7290–7304 (2016)
8. Aigbe, U.O., Osibote, O.A.: A review of hexavalent chromium removal from aqueous solutions by sorption technique using nanomaterials. *J. Environ. Chem. Eng.* 8(6), 104503 (2020)
9. Li, Y., et al.: Influence of biochars on the accessibility of organochlorine pesticides and microbial community in contaminated soils. *Sci. Total Environ.* 647, 551–560 (2018)
10. Weng, X., et al.: Impact of synthesis conditions on Pb(II) removal efficiency from aqueous solution by green tea extract reduced graphene oxide. *Chem. Eng. J.* 359, 976–981 (2019)
11. Massironi, A., et al.: Ulvan as novel reducing and stabilising agent from renewable algal biomass: Application to green synthesis of silver nanoparticles. *Carbohydr. Polym.* 203, 310–321 (2019)
12. Jiang, T.F., Lv, Z.H., Wang, Y.H.: Separation and determination of chalcones from *Carthamus tinctorius* L. and its medicinal preparation by capillary zone electrophoresis. *J. Sep. Sci.* 28(11), 1244–1247 (2005)
13. Salam, M.A.: Preparation and characterisation of chitin/magnetite/multiwalled carbon nanotubes magnetic nanocomposite for toxic hexavalent chromium removal from solution. *J. Mol. Liq.* 233, 197–202 (2017)
14. Sengupta, J., et al.: Physiologically important metal nanoparticles and their toxicity. *J. Nanosci. Nanotechnol.* 14(1), 990–1006 (2014)
15. Bouhrara M., et al.: Magnetically Recoverable Nanocatalysts. *Chem. Rev.* 111(5), 3036–3075 (2011)
16. Deng, Y.H., et al.: Investigation of formation of silica-coated magnetite nanoparticles via sol-gel approach. *Colloids Surfaces. A Physicochem. Eng. Asp.* 262(1–3), 87–93 (2005)
17. Park, Y., et al.: Polysaccharides and phytochemicals: A natural reservoir for the green synthesis of gold and silver nanoparticles. *IET Nanobiotechnol.* 5(3), 69–78 (2011)
18. Philip, D., et al.: *Murraya Koenigii* leaf-assisted rapid green synthesis of silver and gold nanoparticles. *Spectrochim. Acta Part A Mol. Biomol. Spectrosc.* 78(2), 899–904 (2011)
19. Vishnu, D., Dhandapani, B.: Integration of *Cynodon dactylon* and *Murraya koenigii* plant extracts in amino-functionalised silica-coated magnetic nanoparticle as an effective sorbent for the removal of chromium(VI) metal pollutants. *IET Nanobiotechnol.* 14(6), 449–456 (2020)
20. Vishnu, D., et al.: Fabrication of surface-engineered superparamagnetic nanocomposites (Co/Fe/Mn) with biochar from groundnut waste residues for the elimination of copper and lead metal ions. *J. Nanostruct. Chem.* (2020)
21. Vishnu, D., Dhandapani, B., K., S.: The symbiotic effect of integrated *Murraya koenigii* extract and surface-modified magnetic microspheres—a green biosorbent for the removal of Cu(II) and Cr(VI) ions from aqueous solutions. *Chem. Eng. Commun.* 6445 (2019)
22. Nithya, K., Sathish, A., Kumar, P.S.: Packed bed column optimization and modelling studies for removal of chromium ions using chemically modified *Lantana camara* adsorbent. *J. Water Process. Eng.* 33(November2019), 101069 (2020)
23. Nwabanne, J.T., Okoye, A.C., Lebele-Alawa, B.T.: Packed bed column studies for the removal of lead (II) using oil palm empty fruit Bunch. *Eur. J. Sci. Res.* 63(2), 296–305 (2011)
24. Han, R., et al.: Biosorption of methylene blue from aqueous solution by rice husk in a fixed-bed column. *J. Hazard. Mater.* 141(3), 713–718 (2007)
25. Oh, H.-J., et al.: Adsorption of methylene blue by phoenix tree leaf powder in a fixed-bed column: experiments and prediction of breakthrough curves. *Desalination*, 2009, 238, (September 2015), 333–346
26. Zheng, Y.M., et al.: Removal of arsenite from aqueous solution by a zirconia nanoparticle. *Chem. Eng. J.* 188, 15–22 (2012)
27. Yahya, M.D., et al.: Column adsorption study for the removal of chromium and manganese ions from electroplating wastewater using cashew nutshell adsorbent. *Cogent. Eng.* 7(1) 1–18 (2020)
28. Sarma, P.J., Kumar, R., Pakshirajan, K.: Batch and continuous removal of copper and lead from aqueous solution using cheaply agricultural waste materials. *Int. J. Environ. Res.* 9(2), 635–648 (2015)
29. Majumdar, S., Baishya, A., Mahanta, D.: Kinetic and equilibrium modelling of anionic dye adsorption on polyaniline emeraldine salt: batch and fixed bed column studies. *Fibers Polym.* 20(6), 1226–1235 (2019)
30. Chen, S., et al.: Adsorption of hexavalent chromium from aqueous solution by modified corn stalk: a fixed-bed column study. *Bioresour. Technol.* 113, 114–120 (2012)
31. Yahya, M.D., Odigire, J.O.: Fixed bed column study for Pb (II) adsorption using calcium-alginate treated shea butter husk (TSBH). In: 2015. International Conference on Industrial Engineering and Operations Management (IEOM), 1–9. Date of Conference: 3-5 March 2015 Dubai, United Arab Emirates (2015)
32. Chowdhury, Z.Z., et al.: Breakthrough curve analysis for column dynamics sorption of Mn(II) ions from wastewater by using *Mangostana garcinia* peel-based granular-activated carbon. *J. Inside Chem.* 2013(Ii) (2013)
33. Srivastava, S., Agrawal, S.B., Mondal, M.K.: A fixed bed column study of natural and chemically modified *Lagerstroemia speciosa* bark for removal of synthetic Cr(VI) ions from aqueous solution. *Int. J. Phytoremediation.* 22(12), 1233–1241 (2020)
34. Mitra, T., Das, S.K.: Cr(VI) removal from aqueous solution using *Psidium guajava* leaves as green adsorbent: column studies. *Appl. Water Sci.* 9(7), 1–8 (2019)
35. Nag, S., Bar, N., Das, S.K.: Cr(VI) removal from aqueous solution using green adsorbents in continuous bed column – statistical and GA-ANN hybrid modelling. *Chem. Eng. Sci.* 226(VI), 115904 (2020)
36. Beheshti, H., et al.: Removal of Cr (VI) from aqueous solutions using chitosan/MWCNT/Fe₃O₄ composite nanofibers-batch and column studies. *Chem. Eng. J.* 284(VI), 557–564 (2016)
37. Karimi, M., et al.: Column study of Cr (VI) adsorption onto modified silica-polyacrylamide microspheres composite. *Chem. Eng. J.* 210, 280–288 (2012)
38. Vishnu, D., Dhandapani, B.: A review on the Synergetic effect of plant extracts on nanomaterials for the removal of metals in industrial effluents. *Curr. Anal. Chem.* 6, 1573–1580 (2020)

How to cite this article: Vishnu D, Dhandapani B. Evaluation of column studies using *Cynodon dactylon* plant-mediated amino-grouped silica-layered magnetic nanoadsorbent to remove noxious hexavalent chromium metal ions. *IET Nanobiotechnol.* 2021;15:402–410. <https://doi.org/10.1049/nbt2.12029>